European Journal of Medicinal Chemistry 122 (2016) 429–435

Contents lists available at ScienceDirect

European Journal of Medicinal Chemistry

journal homepage: http://www.elsevier.com/locate/ejmech

Short communication

Exploring the readthrough of nonsense mutations by non-acidic Ataluren analogues selected by ligand-based virtual screening

Ivana Pibiri [a], Laura Lentini [a, *], Marco Tutone [a], Raffaella Melfi [a], Andrea Pace [a, b, **], Aldo Di Leonardo [a, c]

[a] Dipartimento di Scienze e Tecnologie Biologiche, Chimiche e Farmaceutiche (STEBICEF), Università degli Studi di Palermo, Viale delle Scienze Ed. 16-17, 90128 Palermo, Italy
[b] Istituto EuroMediterraneo di Scienza e Tecnologia (IEMEST), Via Emerico Amari 123, 90139 Palermo, Italy
[c] Centro di OncoBiologia Sperimentale (COBS), via San Lorenzo Colli, 90145 Palermo, Italy

ARTICLE INFO

Article history:
Received 23 March 2016
Received in revised form
9 June 2016
Accepted 27 June 2016
Available online 29 June 2016

Keywords:
PTCs readthrough
CFTR gene
Nonsense mutation
Oxadiazoles
Cystic fibrosis

ABSTRACT

Ataluren, also known as PTC124, is a 5-(fluorophenyl)-1,2,4-oxadiazolyl-benzoic acid suggested to suppress nonsense mutations by readthrough of premature stop codons in the mRNA. Potential interaction of PTC124 with mRNA has been recently studied by molecular dynamics simulations highlighting the importance of H-bonding and stacking π–π interactions. A series of non-acidic analogues of PTC124 were selected from a large database via a ligand-based virtual screening approach. Eight of them were synthesized and tested for their readthrough activity using the Fluc reporter harboring the UGA premature stop codon. The most active compound was further tested for suppression of the UGA nonsense mutation in the bronchial epithelial IB3.1 cell line carrying the W1282X mutation in the CFTR gene.

1. Introduction

When a premature stop codon is present in the coding region of the mRNA, protein translation is interrupted thus producing truncated polypeptides. This situation is promptly detected by the nonsense mediated mRNA decay (NMD) pathway. The NMD is a surveillance mechanism that targets the cytoplasmic PTC-bearing transcript for rapid degradation [1]. Nonsense mutations are the cause of a significant percentage of most inherited diseases, including cystic fibrosis (CF), Duchenne muscular dystrophy (DMD), Usher's Syndrome, and a variety of other genetic disorders [2–4].

Due to the presence of premature stop codons in their CF *trans*-membrane regulator gene, approximately 10% of CF patients lack adequate levels of the CFTR protein, a chloride channel that is required for normal function of the lung, pancreas, liver, and other organs [5].

Gene therapy, that is potentially a method of choice to correct the mutated gene, is far from clinical routine. Alternative pharmacological approaches aim at modifying gene expression and have been applied to diseases caused by a premature stop codon. Indeed, the translational readthrough of a nonsense mutation might allow the synthesis of a full-length functional protein [6,7]. A well known category of drugs, the antibiotic aminoglycosides (e.g. gentamicin, tobramycin, paromomycin, amikacin, etc.) possess the ability to readthrough stop codons by disturbing the translation machinery and leading to the insertion of a near-cognate amino acid at a PTC [8–11]. However, aminoglycoside readthrough action lacks specificity thus resulting in readthrough of many correctly positioned stop codons, and originating toxic aggregates that after long-term treatments can cause nephrotoxicity and ototoxicity [3,12–14].

3-[5-(2-Fuorophenyl)- [1,2,4]oxadiazol-3-yl]-benzoic acid (also named PTC124 or Ataluren), was developed as a drug capable to promote selectively the readthrough of premature termination codons [6]. Recently, also the antiinflammatory drug amlexanox has been claimed to promote readthrough of nonsense mutations

* Corresponding author.
** Corresponding author. Dipartimento di Scienze e Tecnologie Biologiche, Chimiche e Farmaceutiche (STEBICEF), Università degli Studi di Palermo, Viale delle Scienze Ed. 16-17, 90128 Palermo, Italy.
E-mail addresses: laura.lentini@unipa.it (L. Lentini), andrea.pace@unipa.it (A. Pace).

http://dx.doi.org/10.1016/j.ejmech.2016.06.048
0223-5234/

[15,16]. Overall, the general concept underlying therapeutic nonsense suppression is that a single drug, focused on a specific genetic defect, may be beneficial to different diseases whose common denominator is a nonsense mutation. PTC124 is not structurally similar to aminoglycosides and its activity was first assessed in HEK293 cells transfected with a luciferase gene (LUC190) harboring a premature stop codon at Thr190, replacing the normal ACA with UAA, UAG and UGA. Such ability was also assessed using MDX mice (mice with Duchenne Muscular Dystrophy caused by nonsense mutation) showing 20–25% recovery of full-length dystrophin [6].

In these past years PTC124 has been the subject of an intense debate about its mechanism of action, because some studies evidenced that it has an effective readthrough activity [4] while a few studies did not find enough evidence to prove the readthrough activity of PTC124 [17–19]. Our previous results on readthrough activity of PTC124 tested with a novel reporter vector harboring a premature stop codon (TGA) in the H2B-GFP fused gene (H2B-GFP-*opal*) and a molecular dynamics simulation on the hypothetical interaction between PTC124 and a mRNA fragment supported the hypothesis that PTC124 is able to promote the specific readthrough of internal UGA premature stop codons [20].

Recently, we also reported the synthesis of a set of variously fluorinated PTC124 analogues and their biological screening in the lower airway cell line (IB3.1) revealed three analogues showing comparable or higher activity than PTC124 as readthrough promoters [21].

However, despite recent progress on the topic, the precise biological site targeted by PTC124 is still unknown. This makes impossible to perform docking studies to suggest convenient modifications of the drug in order to improve its activity even against those stop codons for which PTC124 has shown a reduced effect.

In this context, based on biological data already available on some PTC124 analogues we decided to perform a Ligand Based Virtual Screening in order to identify promising PTC124-*like* candidates eventually providing optimized alternatives for readthrough drug development. Selected candidates were synthesized and tested for their readthrough activity of premature termination codons by using FLuc assay and IB3 cell lines.

2. Materials and methods

2.1. Ligand based virtual screening

Twenty PTC-124 analogs [22,23] were chosen to create the starting dataset for the modeling analysis. The dataset structures were processed with the LigPrep [24] software package in order to assign the appropriate protonation states at physiological pH(7.2 ± 0.2), employing the Ionizer option. Conformers were generated through Macro-Model torsional sampling using the OPLS_2005 force field as reported in a previous paper [25]. The pharmacophore modeling study was performed using the Phase software. Phase is a versatile product for pharmacophore perception, structural alignment, activity prediction, and 3D database creation and searching [26]. After the ligands preparation, the pharmacophore model was developed by using a set of pharmacophore features to generate sites for all of the compounds. A standard set of six pharmacophore features were used: hydrogen-bond acceptor (A), hydrogen-bond donor (D), hydrophobic group (H), negatively ionizable (N), positively ionizable (P), and aromatic ring (R); Hypotheses were generated by using a previously validated protocol [27,28]. Virtual high-throughput screening was performed on ZINC "drug-like" database [29], consisting of about $2^{*}10^{6}$ compounds and filtered according to the Lipinski's rule of Five [30].

2.2. Chemistry

All solvents and reagents were obtained from commercial sources. All synthesized compounds were purified by chromatography and analyzed by IR, HRMS, and NMR. Purity of synthesized compounds was verified prior to biological tests by chromatographic analyses and NMR (see supplementary material) and in all the cases purity was higher than 95%. IR spectra have been registered (in Nujol) with a Shimadzu FTIR-8300 spectrophotometer; melting points have been determined on a Reichart-Thermovar hotstage Kofler and are uncorrected. NMR spectra have been registered on a Bruker AVANCE DMX 300 using $CDCl_3$ and DMSO as solvent. HRMS spectra were recorded by analyzing a 50 ppm solution of the compound in a 6540 UHD Accurate-Mass Q-TOF LC/MS (Agilent Technologies) equipped with a Dual AJS ESI source. GC-MS spectra have been registered by using either an Agilent 7890B/7000C GC-MS-TQ or a GC-MS Shimadzu QP-2010 Instrument. Flash chromatography was performed by using silica gel (Merck, 0.040–0.063 mm) and mixtures of ethyl acetate and petroleum ether (fraction boiling in the range of 40–60 °C) in various ratios. 3-Methyl-benzamidoxime [31], 2-picolin-amidoxime [32], isonicotin-amidoxime [33], nicotin-amidoxime [33], and benzamidoxime [34] were synthesized as reported. Generally, an acqueous solution of hydroxylamine was prepared by mixing $NH_2OH^{*}HCl$ (36 mmol) and NaOH (36 mmol) in water (20 mL). The hydroxylamine solution was then added to an alcoholic solution of the corresponding nitrile (30 mmol) dissolved in ethanol (100 mL) in a 250 mL round bottomed flask. The mixture was refluxed for 8 h. The solvent was then removed under vacuum and 100 mL water were added to the residue. The amidoxime was filtered as a white solid and re-crystallized from ethanol.

2.2.1. General procedure for the synthesis of 1,2,4-oxadiazoles

The synthesis of 1,2,4-oxadiazoles has been performed by the amidoxime route [35]. The appropriate amidoxime (0.3 g) was dissolved in 50 mL of toluene in a 250 mL round bottomed flask. Then, 1.2 eq. of the appropriate aroyl chloride and 1.2 eq. of pyridine were added and the reaction mixture was refluxed for 6–8 h monitoring the reaction by TLC until consumption of starting material. The solvent was removed under vacuum and water was added to the residue. Extraction with ethyl acetate and chromatographic separation on silica gel using mixtures of petroleum ether and ethyl acetate as eluent allowed to obtain the desired oxadiazole, further purified by crystallization.

3-(2′-pyridyl)-5-(3′-cyanophenyl)-1,2,4-oxadiazole (NV1859). (0.49 g; 89% Yield). White solid, m.p. 148–149 °C from petroleum ether (lit. [36].148–149 °C). ^{1}H NMR (300 MHz, $CDCl_3$): δ (ppm) 8.86 (dd, 1H, J_1 = 10.0 Hz, J_2 = 4.8 Hz), 8.60 (brs, 1H), 8.52 (1H, d, J = 8.0 Hz), 8.23 (1H, d, J = 8.0 Hz), 7.90 (2H, m), 7.73 (1H, t, J = 7.8 Hz), 7.49 (1H, dd, J_1 = 8.0 Hz, J_2 = 4.8 Hz); ^{13}C NMR (75 MHz, $CDCl_3$): δ (ppm) 174.38, 169.01, 150.55, 145.93, 137.19, 135.88, 132.07, 131.75, 130.22, 125.82, 125.30, 123.36, 117.34, 113.88; HRMS for $C_{14}H_8N_4O$ found 249.0782 $[M+H]^+$ (Calcd. 249.0771).

3-(4′-pyridyl)-5-(3′-toluyl)-1,2,4-oxadiazole(NV1861). (0.32 g; 62% Yield). White solid, m.p. 109–110 °C from petroleum ether (lit. [37]. 111–112 °C). ^{1}H NMR (300 MHz, $CDCl_3$): δ (ppm) 8.78 (d, 2H, J = 5.5 Hz), 8.00–7.92 (m, 4H), 7.42 (d, 2H, J = 5.5 Hz), 2.45 (s, 3H); ^{13}C NMR (75 MHz, $CDCl_3$): δ (ppm) 177.40, 168.00, 151.09, 139.87, 135.38, 134.65, 129.80, 129.38, 126.06, 124.37, 122.09, 21.99; HRMS for $C_{14}H_{11}N_3O$ found 238.0989 $[M+H]^+$ (Calcd. 238.0975).

3-(3′-pyridyl)-5-(3′-toluyl)-1,2,4-oxadiazole (NV1879). (0.46 g; 88% Yield)White solid, m.p. 101–102 °C from petroleum ether. ^{1}H NMR (300 MHz, $CDCl_3$): δ (ppm) 9.42 (d, 1H, J = 1.8 Hz), 8.78 (dd, 1H, J_1 = 5.0 Hz, J_2 = 1.8 Hz), 8.46 (dd, 1H, J_1 = 7.9 Hz, J_2 = 1.8 Hz), 8.05 (m, 2H), 7.47 (m, 3H), 2.49 (s, 3H); ^{13}C NMR

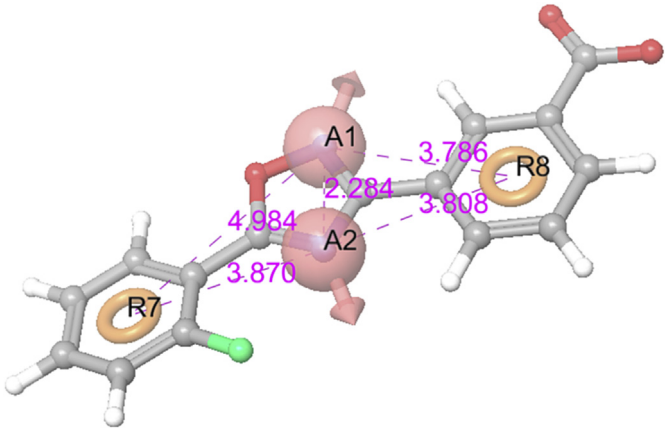

Fig. 1. Best pharmacophore hypothesis AARR.5 aligned with PTC-124.

(75 MHz, $CDCl_3$): δ (ppm) 176.37, 166.96, 151.89, 148.66, 139.13, 134.79, 133.82, 129.07, 128.70, 125.38, 123.86, 123.63, 123.39, 21.37; HRMS for $C_{14}H_{11}N_3O$ found 238.0986 $[M+H]^+$ (Calcd. 238.0975).

3-(3′-phenyl)-5-(3′-toluyl)-1,2,4-oxadiazole(NV1883). (0.44 g; 84% Yield)White solid, m.p. 70–71 °C from petroleum ether (lit. [38]. 74-5 °C). ^1H NMR (300 MHz, $CDCl_3$): δ (ppm) 8.21–8.17, (m, 2H), 8.06–8.00 (m, 2H), 7.54–7.49 (m, 3H), 7.43–7.38 (m, 2H), 2.49 (s, 3H); ^{13}C NMR (75 MHz, $CDCl_3$): δ (ppm) 175.92, 168.94, 150.72, 149.92, 139.02, 133.53, 131.13, 129.00, 128.83, 128.67, 127.54, 127.09, 125.33, 124.25, 21,39; HRMS for $C_{15}H_{14}N_2O$ found 237.1037 $[M+H]^+$ (Calcd. 237.1022).

3-(3-toluyl), 5-(2-toluyl)-1,2,4-oxadiazole (NV1894). (0.46 g; 92% Yield) White solid, m.p. 43–45 °C from petroleum ether. ^1H NMR (300 MHz, $CDCl_3$): δ (ppm) 8,18 (d, 1H, $J = 7.3$ Hz), 7.99 (d, 2H, $J = 7.9$ Hz), 7.45 (m, 5H), 2.80 (s, 3H), 2.47 (s, 3H); ^{13}C NMR (75 MHz, $CDCl_3$): δ (ppm) 176.98, 169.40, 139.80, 139.29,132.80, 132.50, 132.55, 130.90, 129.44, 128.76, 127.74, 126.93, 125.39, 124.27, 22.61, 22.00; HRMS for $C_{16}H_{14}N_2O$ found 251.1195 $[M+H]^+$ (Calcd. 251.1179).

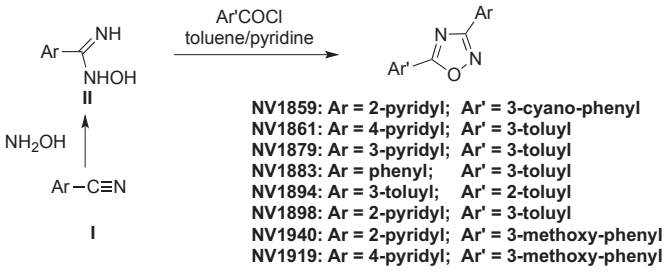

Scheme 1. Amidoxime route toward PTC124 analogues.

3-(2-pyridyl)-5-(3′-toluyl)-1,2,4-oxadiazole (NV1898). (0.47 g; 91% Yield) White solid, m.p. 127–129 °C from petroleum ether. ^1H NMR (300 MHz, $CDCl_3$): δ (ppm) 8.86 (d, 1H, $J = 4.4$ Hz), 8.24 (d, 1H, $J = 8.1$ Hz), 8.22 (s, 1H), 8.12 (m, 1H), 7.89 (m, 1H), 7.59 (m, 3H), 2.47 (s, 3H); ^{13}C NMR (75 MHz, $CDCl_3$): δ (ppm) 176.65, 168.71, 150.39, 146.53, 139.01, 137.00, 133.71, 128.96, 128.87, 125.40, 125.45, 123.89, 123.21,21.27; HRMS for $C_{14}H_{11}N_3O$ found 238.0952 $[M+H]^+$ (Calcd. 238.0975).

3-(2-pyridyl)-5-(3′-anisoyl)-1,2,4-oxadiazole (NV1940). (0.47 g; 84% Yield)White solid, m.p. 100–102 °C from petroleum ether. ^1H NMR (300 MHz, $CDCl_3$): δ (ppm) 8.86 (d, 1H, $J = 4.4$ Hz), 8.24 (d, 1H, $J = 7.9$ Hz), 7.89 (m, 2H), 7.80 (brs, 1H), 7.47 (t, 2H, $J = 7.9$ Hz), 7.17 (dd, 1H, $J_1 = 7.9$ Hz, $J_2 = 2.5$ Hz), 3.92 (s, 3H); ^{13}C NMR (75 MHz, $CDCl_3$): δ (ppm) 177.17, 169.47, 160.73, 151.15, 147.20, 137.77, 130.90, 126.21, 124.00, 121.49, 120.50, 113.32, 56.34, 30.36; HRMS for $C_{14}H_{11}N_3O_2$ found 254.0921 $[M+H]^+$ (Calcd. 254.0924).

3-(4′-pyridyl)-5-(3′-anisoyl)-1,2,4-oxadiazole (NV1919). (0.51 g; 91% Yield) White solid, m.p. 123–125 °C from petroleum ether. ^1H NMR (300 MHz, $CDCl_3$): δ (ppm) 8.84 (d, 2H, $J = 7.5$ Hz), 8.14 (d, 2H, $J = 7.5$ Hz), 7.83 (brd, 1H, $J = 8.0$ Hz), 7.73 (brs, 1H), 7.50 (1H, t, $J = 8.0$ Hz), 7.19 (dd, 1H, $J_1 = 8.0$ Hz, $J_2 = 2.5$ Hz), 3.94 (s, 3H); ^{13}C NMR (75 MHz, $CDCl_3$): δ (ppm) 176.45, 167.40, 160.06, 150.50, 134.56, 130.35, 124.90, 121.38, 120.63, 119.57, 112.79, 55.56; HRMS for $C_{14}H_{11}N_3O_2$ found 254.0907 $[M+H]^+$ (Calcd. 254.0924).

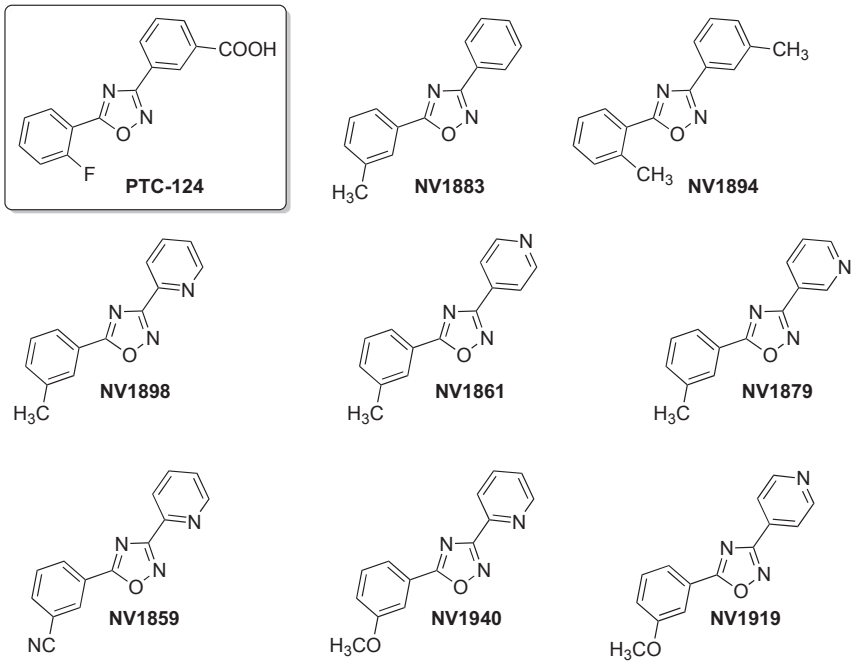

Fig. 2. PTC124 and selected analogues from the top 5% of virtual screening hits.

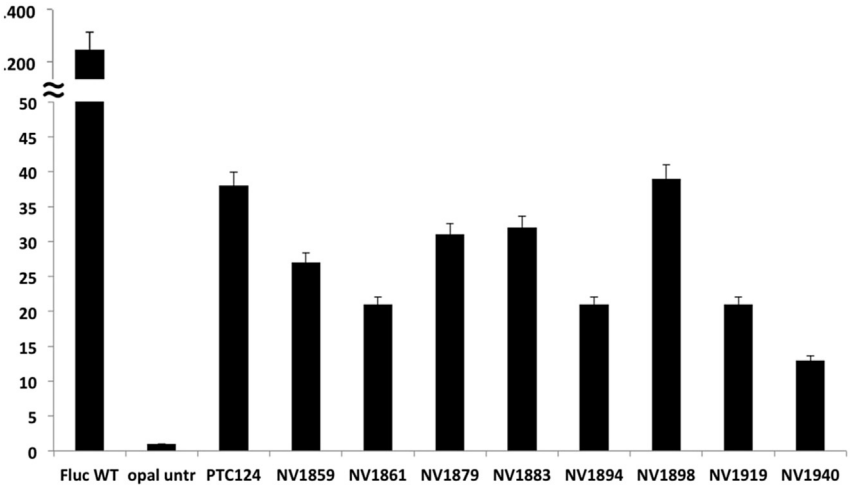

Fig. 3. Luciferase activity of HeLa FLuc190^{UGA} transfected cells after treatment with PTC124 and its analogues compared to that of untreated (opal untr) and untransfected (Fluc WT) cells.

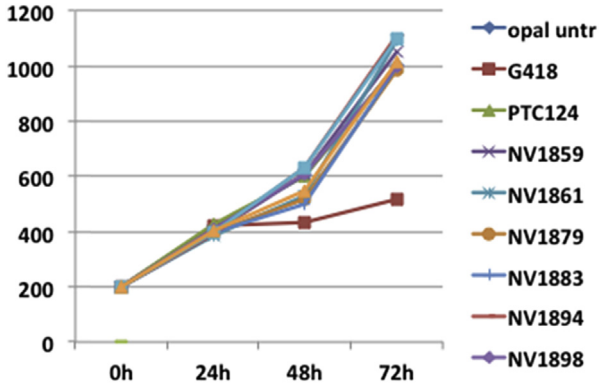

Fig. 4. Cell viability assay of HeLa cells after 24, 48, and 72 h treatment with G418, PTC124, and PTC124 analogues (Control: opal untreated cells).

2.3. Biology

2.3.1. Cell culture conditions and transfection of reporter plasmid

HeLa, CFBE41o- (expressing ectopic CFTR-WT, were kindly provided by Prof. Louis Galietta, Ospedale Gaslini-Genova, Italy) and IB3.1 cells were cultured in DMEM supplemented with FBS 10% (GIBCO) in a humidified atmosphere of 5% CO_2 in air at 37 °C.

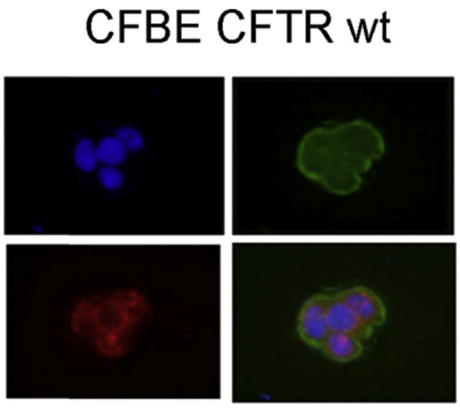

Fig. 5. Immunofluorescence assay showing the CFTR protein in CFBE41o-cells. Nuclei (Top left), CFTR localization (Top right), Membrane and Golgi apparatus (Bottom left) and merged images (Bottom right).

2.3.2. Measurement of luciferase activity by luminescence

HeLa cells plated in a 6 well plate at a density of 2×10^5/ml were transfected with WT (Fluc) and mutant (Fluc-*opal*) plasmids, by using lipofectamine 2000 (Invitrogen). Cells were incubated for 24 h and PTC124 and the others compounds (12 μM) were added for additional 24 h. Next, cells were washed with PBS, incubated with the detection mix Steady-Glo luciferase reagent (Promega) and 200 μl of cell suspension were plated in triplicate in a 96 well plate. Luciferase activity was measured on a luminometer (Promega).

2.3.3. Cell viability assay

2×10^5/ml HeLa cells were plated and incubated with PTC124 (12 μM), G418 (300 μg/mL) and PTC124 analogues (12 μM). Cells were counted every 24 h during the treatments (for a total of 72 h) and the results reported in a graph.

2.3.4. Immunofluorescence microscopy

To visualize the CFTR protein, cells were grown on rounded glass coverslips and fixed with methanol for 2 min. The cell membrane and Golgi apparatus were stained by the Wheat Germ Agglutinin (WGA) Alexa 594 (Life Technologies). Coverslips were incubated with a mouse monoclonal antibody (CF3) that recognizes the first extracellular loop of human CFTR (Abcam, 1:500) overnight at 4 °C, followed by a goat polyclonal to mouse Alexa-Fluor-488 (Abcam, 1:1000) secondary antibody for 1 h at 37 °C. Nuclei were visualized with DAPI. Cells were examined under a Zeiss Axioskop microscope equipped for fluorescence.

2.3.5. Western blotting

Proteins (50 μg) were separated by 10% SDS-PAGE and 4–12% SDS-PAGE containing 0.1% SDS and transferred to Hybond-C nitrocellulose membranes (Amersham Life Science) by electro-blotting. The membrane was incubated with a goat polyclonal antibody anti–CFTR (C-19, Santa Cruz 1:500) raised against a peptide mapping near the C-terminus of CFTR of human origin, and HRP-conjugated anti-goat (Abcam, 1:5000). The target protein was detected by ECL reagents (Pierce). We used β-tubulin antibody (mouse; Sigma-Aldrich 1:10.000) to confirm equal proteins loading. Gel bands were quantified by Image Lab software (BioRad).

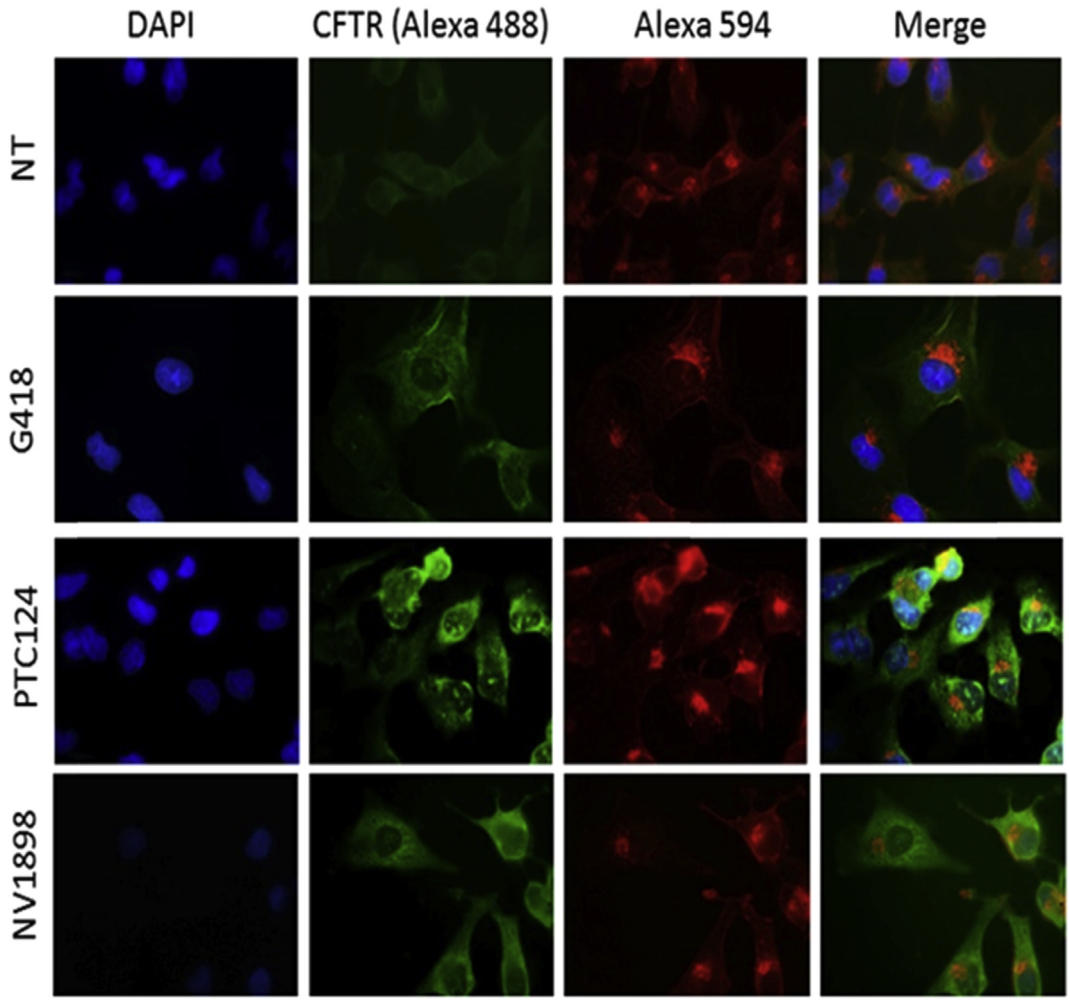

Fig. 6. Immunofluorescence assay showing Nuclei (blue), CFTR (green), cell membrane and Golgi apparatus (red) and the corresponding merged images to detect readthrough of the CFTR's UGA premature stop codon in IB3.1 human cells untreated (NT) or treated for 24 h with G418 (positive control), PTC124 and **NV1898**. (For interpretation of the references to colour in this figure legend, the reader is referred to the web version of this article.)

3. Results and discussion

The original report on the activity of PTC124 highlighted the selectivity of such a small molecule toward the readthrough of premature UGA codon, also pointing out the dependence of the activity on the identity of the nucleobases surrounding the PTC. More recently, the importance of H-bonding and $\pi-\pi$ stacking interactions between the PTC124 and its hypothetical target have been remarked. The inactivity of a very similar set of PTC124 analogues and the finding of analogues with improved activity prompted us to explore a ligand-based virtual screening approach in attempting to optimize the structure of PTC124-*like* compounds.

The used dataset for the pharmacophore modeling study consisted of PTC124 and twenty PTC124 analogs. Among the latter, the ten compounds showing no readthrough activity, and the other ten known to give artifacts in luciferase activity assays, were identified as inactive compounds, while PTC-124 was identified as the active compound. The scoring protocol allowed the different hypotheses to be ranked so that the most appropriate can be chosen for further investigation. Inactive molecules were scored, in order to observe the alignment of these molecules with the pharmacophore hypotheses and to select the best ones. The larger the difference between the scores of the active and inactive molecules, the better the hypothesis is at discriminating among candidates. Thirteen four-point pharmacophore variants were retrieved: seven AHRR and six AARR variants, where R indicates aromatic rings, while A and H are H-bond acceptor and donor sites, respectively. Six pharmacophore hypothesis survived the scoring protocol and the best one was AARR.5 as shown in Fig. 1.

Such hypothesis is represented by two aromatic rings (R7 and R8) distant 7.67 Å from each other and separated by two hydrogen bond acceptors (A1 and A2) at a distance of 2.28 Å from each other. A1 is distant 4.98 Å and 3.79 Å from R7 and R8, respectively, while A2 is distant 3.87 Å and 3.08 Å from R7 and R8, respectively. It is quite surprising to note that no particular role is assigned to the fluorine and carboxylic moiety by the scoring protocol, proposing the diaryl azole as the main scaffold and suggesting only an ancillary role of the substituents on the aryl rings.

A virtual high-throughput screening was carried out by matching the AARR.5 pharmacophore model with compounds contained in the drug-like subset of ZINC database. By optimizing the diaryloxadiazole scaffold, a set of 250 compounds was filtered by the virtual screening of the initial database. From the top 5% of retrieved hits in term of fitness with the hypothesis, eight compounds (Fig. 2) were selected to be synthesized and tested for readthrough activity. Interestingly, although still belonging to the class of 3,5-diaryl-1,2,4-oxadiazoles, none of the selected hits contained the two main features of PTC124 lead, i.e. the fluorine

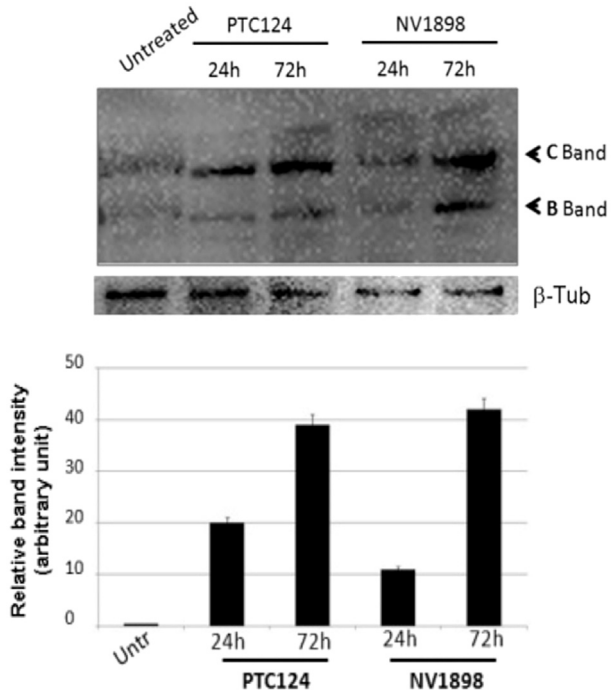

Fig. 7. Western blot showing CFTR protein levels in IB3.1 cells untreated (untr.) or treated with PTC124 or NV1898. A primary antibody targeting the C-terminus of CFTR was used, β-tubulin was used as a loading control (Top). Graph shows the quantitation of the bands by densitometry using the Image Lab software (BioRad) (Bottom).

substituent and the carboxylic moiety.

Selected hits were then synthesized in good to excellent yields (62–92%) by cyclization of arylamidoximes **II**, prepared from the corresponding nitriles **I** and hydroxylamine, with variously substituted benzoyl chloride, appropriately chosen according to the required substitution pattern (Scheme 1).

The readthrough activity of synthesized compounds was preliminarily assessed by using the FLuc cell-based assay (Fig. 3) [8]. To this aim HeLa cells were transiently transfected with the plasmids pFLuc-WT and pFLuc-*opal* plasmids, and Luciferase activity was measured by luminescence. The dose used (12 μM) was chosen on the basis of previous results on similar compounds. Detection of high levels of luciferase activity showed by HeLa cells transfected with the pFLuc-WT plasmid indicated the correct functioning of this assay.

Cell viability (Fig. 4) experiments conducted for a total of 72 h showed that all the PTC124 analogues were significantly less cytotoxic, at the active dose, than G418 chosen as control.

The 3-(2-pyridyl)-5-(3-toluyl)-1,2,4-oxadiazole (**NV1898**) showed readthrough activity comparable to that of PTC124. Considering the basic nature of the pyridyl moiety, this result reinforces the hypothesis that the 3-aryl moiety on the 1,2,4-oxadiazole ring is involved as H-bond acceptor in the interaction with the biological target, as observed in our previous molecular dynamic study on PTC124.

The activity of **NV1898** was then tested for suppression of nonsense mutations in the CF bronchial epithelial IB3.1 cell line (CFTR genotype W1282X/F508del). As a positive control for the CFTR protein expression we used CFBE41o-cells that express ectopically a wild type CFTR gene. The CFTR protein was revealed (green) by a specific antibody targeting its first external loop (Alexa-488). Nuclei were DAPI stained (blue) while the cell membrane and Golgi apparatus were stained with WGA-Alexa-594 (red) (Fig. 5).

Detection of increased level of the CFTR protein (Fig. 6) by immunofluorescence microscopy confirmed that the **NV1898** compound was able to readthrough the UGA premature stop codon inducing the re-expression of CFTR and its localization on the membrane of human IB3.1 cells.

In addition, western blot analysis indicated increased CFTR expression after 24–72 h of treatment with **NV1898** (Fig. 7; top). Quantitation of the band intensity (Fig. 7; bottom) demonstrates similar CFTR protein expression levels between PTC124 and **NV1898** treated cells at 72 h.

4. Conclusions

The so called “small molecule” strategy to promote the readthrough of premature termination codons is currently focused on two types of molecules, i.e. aminoglycosides and diaryloxadiazoles, although recent findings have pointed out at the potential role in nonsense mutation suppressing by the antiinflammatory drug amlexanox. However, PTC124 is both structurally and dimensionally different from aminoglycosides, for which a mechanistic hypothesis has been proved. Therefore, there is still an urgent need for data concerning the structure-activity relationship (SAR) of the PTC124 scaffold, in order to provide a likely hypothesis for PTC124 mode of action thus opening the way to further drug development. Indeed, despite the pioneering original study nature has extensively tested several hundred thousands of compounds finally leading to select PTC124 on the basis of FLuc assays, the possibility to optimize such compound is not precluded. Recently, the SAR of diaryl-1,2,4-oxadiazoles has been investigated mainly by focusing on the number and position of fluorine substituents on the C(5)-linked aromatic ring. The present work represents the first systematic approach of computer driven drug design applied through the ligand based virtual screening of a series of PTC124 analogues. Although not presenting an original scaffold, our study demonstrates the possibility of designing and obtaining alternative PTC124 analogues with similar activity, even in the absence of the fluorine and carboxylic moieties. The used approach is particularly valid in the absence of a known biological target, and is iteratively improvable by implementing bioactivity data of the synthesized compounds into the pharmacophoric dataset.

Conflict of interest

The authors declare that they have no conflict of interest.

Authors contribution

All authors have contributed to this article and particularly I. Pibiri and L. Lentini have contributed equally.

Acknowledgments

This work was funded by the Italian Cystic Fibrosis Research Foundation, grant FFC#02/2011 to Prof. Aldo Di Leonardo with the contribution of Delegazione di Lecce and Delegazione di Vittoria (Ragusa); FFC#1/2014 to Dr. Laura Lentini, with the contribution of Delegazione di Palermo, Catania 2 and Vittoria (Ragusa). We thank Prof. Jhon P. Clancy (Cincinnati Children’s Hospital Medical Center, OHIO-USA) and Prof. Louis Galietta (Ospedale Gaslini Genova), for respectively producing and providing us with CFBE41o-cells. We are also grateful to Prof. J. Inglese (NIH Chemical Genomics Center, National Institutes of Health, Bethesda) for kindly providing us with the FLuc190^{UGA} plasmid.

Appendix A. Supplementary data

Supplementary data related to this article can be found at http://dx.doi.org/10.1016/j.ejmech.2016.06.048.

References

[1] S. Kervestin, A. Jacobson, NMD: a multifaceted response to premature translational termination, Nat. Rev. Mol. Cell Biol. 13 (2012) 700–712.
[2] J.T. Mendell, H.C. Diez, When the message goes awry: disease-producing mutations that influence mRNA content and performance, Cell 107 (2001) 411–414.
[3] L. Bidou, V. Allamand, J.P. Rousset, O. Namy, Sense from nonsense: therapies for premature stop codon diseases, Trends Mol. Med. 18 (2012) 679–688.
[4] T. Goldmann, N. Overlack, F. Moller, V. Belakhov, M. van Wyk, T. Baasov, U. Wolfrum, K. Nagel-Wolfrum, A comparative evaluation of NB30, NB54 and PTC124 in translational read-through efficacy for treatment of an USH1C nonsense mutation, EMBO Mol. Med. 4 (2012) 1186–1199.
[5] I. Sermet-Gaudelus, K.D. Boeck, G.J. Casimir, F. Vermeulen, T. Leal, A. Mogenet, D. Roussel, J. Fritsch, L. Hanssens, S. Hirawat, N.L. Miller, S. Constantine, A. Reha, T. Ajayi, G.L. Elfring, L.L. Miller, Ataluren (PTC124) induces cystic fibrosis transmembrane conductance regulator protein expression and activity in children with nonsense mutation cystic fibrosis, Am. J. Respir. Crit. Care Med. 182 (2010) 1262–1272.
[6] E.M. Welch, E.R. Barton, J. Zhuo, Y. Tomizawa, W.J. Friesen, P. Trifillis, S. Paushkin, M. Patel, C.R. Trotta, S. Hwang, R.G. Wilde, G. Karp, J. Takasugi, G. Chen, S. Jones, H. Ren, Y.C. Moon, D. Corson, A.A. Turpoff, J.A. Campbell, M.M. Conn, A. Khan, N.G. Almstead, J. Hedrick, A. Mollin, N. Risher, M. Weetall, S. Yeh, A.A. Branstrom, J.M. Colacino, J. Babiak, W.D. Ju, S. Hirawat, V.J. Northcutt, L.L. Miller, P. Spatrick, F. He, M. Kawana, H. Feng, A. Jacobson, S.W. Peltz, H.L. Sweeney, PTC124 targets genetic disorders caused by nonsense mutations, Nature 447 (2007) 87–91.
[7] S.M. Rowe, J.P. Clancy, Pharmaceuticals targeting nonsense mutations in genetic diseases, Biodrugs 23 (2009) 165–174.
[8] D. Diop, C. Chauvin, O. Jean-Jean, Aminoglycosides and other factors promoting stop codon readthrough in human cells, C. R. Biol. 330 (2007) 71–79.
[9] T. Hermann, Aminoglycoside antibiotics: old drugs and new therapeutic approaches, Cell. Mol. Life. Sci. 64 (2007) 1841–1852.
[10] L.S. Mc Coy, Y. Xie, Y. Tor, Antibiotics that target protein synthesis, Wiley Interdiscip. Rev. RNA 2 (2011) 209–232.
[11] V. Malik, L.R. Rodino-Klapac, L. Viollet, J.R. Mendell, Aminoglycoside-induced mutation suppression (stop codon read- through) as a therapeutic strategy for Duchenne muscular dystrophy, Ther. Adv. Neurol. Disord. 3 (2010) 379–389.
[12] N.T. Chandrika, S. Garneau-Tsodikova, A review of patents (2011–2015) towards combating resistance to and toxicity of aminoglycosides, Med. Chem. Commun. 7 (2016) 50–68.
[13] J. Karijolich, Y.T. Yu, Therapeutic suppression of premature termination codons: mechanisms and clinical considerations (Review), Int. J. Mol. Med. 34 (2014) 355–362.
[14] A. Prayle, A.R. Smyth, Aminoglycoside use in cystic fibrosis: therapeutic strategies and toxicity, Curr. Opin. Pulm. Med. 16 (2010) 604–610.
[15] J.A. Loudon, Repurposing amlexanox as a 'run the red light cure-all' with readthrough-a 'no-nonsense' approach to personalised medicine, J. Bioanal. Biomed. 5 (2013) 79–96.
[16] J.A. Loudon, Preventing and correcting communicable and non-communicable chronic disease via amlexanox-Dual 'no-nonsense' and inflammatory axis targeting, J. Bioanal. Biomed. 5 (2013) 138–179.
[17] P.K. Dranchak, E. Di Pietro, A. Snowden, N. Oesch, N.E. Braverman, S.J. Steinberg, J.G. Hacia, Nonsense suppressor therapies rescue peroxisome lipid metabolism and assembly in cells from patients with specific PEX gene mutations, J. Cell Biochem. 112 (2011) 1250–1258.
[18] S.C. Harmer, J.S. Mohal, D. Kemp, A. Tinker, Readthrough of long-QT syndrome type 1 nonsense mutations rescues function but alters the biophysical properties of the channel, Biochem. J. 443 (2012) 635–642.
[19] S.P. McElroy, T. Nomura, L.S. Torrie, E. Warbrick, U. Gartner, G. Wood, W.H. McLean, A lack of premature termination codon read-through efficacy of PTC124 (Ataluren) in a diverse array of reporter assays, PLoS Biol. 11 (2013) 1001593.
[20] L. Lentini, R. Melfi, A. Di Leonardo, A. Spinello, G. Barone, A. Pace, A. Palumbo Piccionello, I. Pibiri, Towards a rationale for the PTC124 (Ataluren) promoted read-through of premature stop codons: a computational approach and GFP-reporter cell-based assay, Mol. Pharm. 11 (2014) 653–664.
[21] I. Pibiri, L. Lentini, R. Melfi, G. Gallucci, A. Pace, A. Spinello, G. Barone, A. Di Leonardo, Enhancement of premature stop codon readthrough in the CFTR gene by Ataluren (PTC124) derivatives, Eur. J. Med. Chem. 101 (2015) 236–244.
[22] D.S. Auld, N.T. Southall, A. Jadhav, R.L. Johnson, D.J. Diller, A. Simeonov, C.P. Austin, J. Inglese, Characterization of chemical libraries for luciferase inhibitory activity, J. Med. Chem. 51 (2008) 2372–2386.
[23] D.S. Auld, N. Thorne, W.F. Maguire, J. Inglese, Mechanism of PTC124 activity in cell-based luciferase assays of nonsense codon suppression, Proc. Natl. Acad. Sci. U. S. A. 106 (2009) 3585–3590.
[24] Ligprep V. 2.3, Schrodinger LLC, New York, 2009.
[25] A.M. Almerico, M. Tutone, A. Lauria, Receptor-guided 3D-QSAR approach for the discovery of c-kit tyrosine kinase inhibitors, J. Mol. Model. 18 (2012) 2885–2895.
[26] Phase V. 3.1, Schrodinger LLC, New York, 2009.
[27] A.M. Almerico, M. Tutone, L. Pantano, A. Lauria, A3 adenosine receptor: homology modeling and 3D-QSAR studies, J. Mol. Graph. Model 42 (2013) 60–72.
[28] A. Lauria, M. Ippolito, M. Fazzari, M. Tutone, F. Di Blasi, F. Mingoia, A.M. Almerico, IKK-beta inhibitors: an analysis of drug-receptor interaction by using molecular docking and pharmacophore 3D-QSAR approaches, J. Mol. Graph. Model 29 (2010) 72–81.
[29] J.J. Irwin, B.K. Sholchet, Zinc – a free database of commercially available compounds for virtual screening, J. Chem. Inf. Model 45 (2005) 177–182.
[30] C.A. Lipinski, F. Lombardo, B.W. Dominy, P.J. Feeney, Experimental and computational approaches to estimate solubility and permeability in drug discovery and development settings, Adv. Drug Deliv. Rev. 46 (2001) 3–26.
[31] R.M. Srivastava, M.N. Ramos, L.M. Mendes e Silva, Synthesis, spectroscopic studies and molecular orbital calculations of O-acylbenzamidoximes, Gazz. Chim. Ital. 113 (1983) 845–850.
[32] K. Gobis, H. Foks, A. Kedzia, M. Wierzbowska, Z. Zwolska, Synthesis and antibacterial activity of novel pyridine and pyrazine derivatives obtained from amidoximes, J. Heterocycl. Chem. 46 (2009) 1271–1279.
[33] R. Delaby, P. Reynaud, T. Tupin, Pyridine amidines and amidoximes, Bull. Soc. Chim. Fr. (1957) 714–717.
[34] P. Krüger, Ueber Abkömmlinge des Benzenylamidoxims, Ber. Dtsch. Chem. Ges. 18 (1885) 1055–1060.
[35] A. Pace, P. Pierro, The new era of 1,2,4-oxadiazoles, Org. Biomol. Chem. 7 (2009) 4337–4348.
[36] D. Grant, R. Dahl, N.D. Cosford, Rapid multistep synthesis of 1,2,4-Oxadiazoles in a single continuous microreactor sequence, J. Org. Chem. 73 (2008) 7219–7223.
[37] M.F. Brana, J.M. Castellano, M.J.R. Yunta, Synthesis of 5-aryl-3-(4-pyridyl)-1,2,4-oxadiazoles, J. Heterocycl. Chem. 20 (1983) 1403–1405.
[38] G. Leandri, M. Pallotti, Diazofurans. Ann. Chim. 47 (1957) 376–384.